In the format provided by the authors and unedited.

Targeted repair of heart injury by stem cells fused with platelet nanovesicles

Junnan Tang[1,2,3], Teng Su [1,2], Ke Huang[1], Phuong-Uyen Dinh[1], Zegen Wang[4], Adam Vandergriff[1,2], Michael T. Hensley[1,2], Jhon Cores[1,2], Tyler Allen[1], Taosheng Li[5], Erin Sproul[2], Emily Mihalko[2], Leonard J. Lobo[6], Laura Ruterbories[7], Alex Lynch[7], Ashley Brown[2], Thomas G. Caranasos[8], Deliang Shen[1,2,3], George A. Stouffer[9], Zhen Gu[2], Jinying Zhang[3] and Ke Cheng[1,2,4,10]*
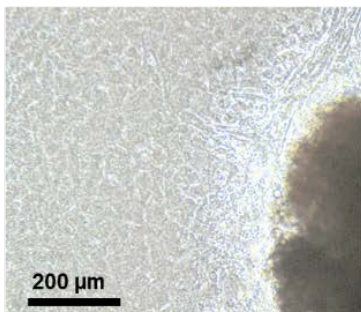
[1]Department of Molecular Biomedical Sciences and Comparative Medicine Institute, North Carolina State University, Raleigh, NC, USA. [2]Joint Department of Biomedical Engineering and Comparative Medicine Institute, University of North Carolina at Chapel Hill & North Carolina State University, Raleigh, NC, USA. [3]Department of Cardiology, The First Affiliated Hospital of Zhengzhou University, Zhengzhou, Henan, China. [4]The Cyrus Tang Hematology Center, Soochow University, Suzhou, Jiangsu, China. [5]Department of Stem Cell Biology, Atomic Bomb Disease Institute, Nagasaki University, Nagasaki, Japan. [6]Division of Pulmonary Diseases and Critical Care Medicine, University of North Carolina at Chapel Hill, Chapel Hill, NC, USA. [7]Department of Clinical Sciences, North Carolina State University, Raleigh, NC, USA. [8]Division of Cardiothoracic Surgery, University of North Carolina at Chapel Hill, Chapel Hill, NC, USA. [9]Division of Cardiology, University of North Carolina at Chapel Hill, Chapel Hill, NC, USA. [10]Pharmacoengineering and Molecular Pharmaceutics Division, Eshelman School of Pharmacy, University of North Carolina at Chapel Hill, Chapel Hill, NC, USA. Junnan Tang, Teng Su, Ke Huang and Phuong-Uyen Dinh contributed equally to this work. *e-mail: ke_cheng@ncsu.edu; ke_cheng@unc.edu

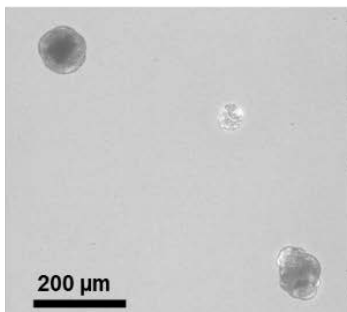# Supplementary Figures and Tables

Targeted repair of heart injury by stem cells fused with platelet nanovesicles

Junnan Tang [1, 2, 3, #], Teng Su[1,2, #], Ke Huang[1, #], Phuong-Uyen Dinh [1, #], Zegen Wang [4], Adam Vandergriff [1, 2], Michael T. Hensley [1, 2], Jhon Cores [1,2], Tyler Allen [1], Taosheng Li [5], Erin Sproul [2], Emily Mihalko [2], Leonard J. Lobo [6], Laura Ruterbories [7], Alex Lynch [7], Ashely Brown [2], Thomas George Caranasos [8], Deliang Shen[1,2,3], George Andrew Stouffer[9], Zhen Gu[2], Jinying Zhang[3], Ke Cheng *[1, 2, 4, 10]
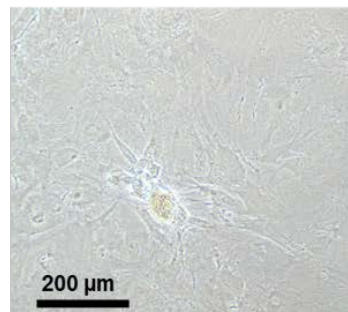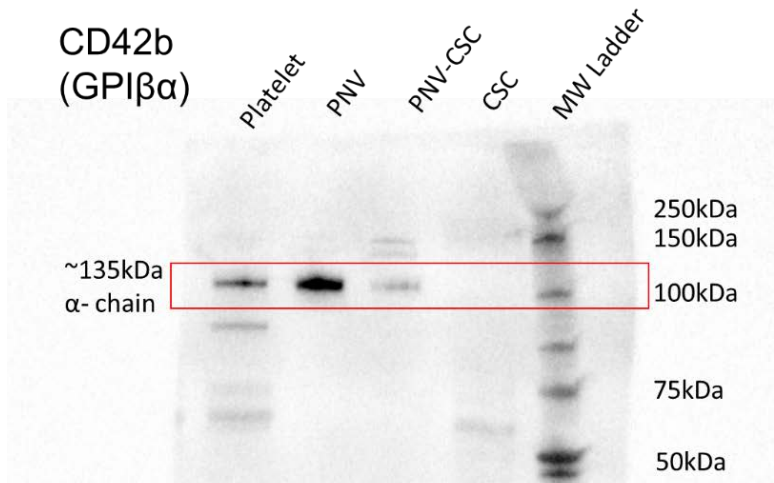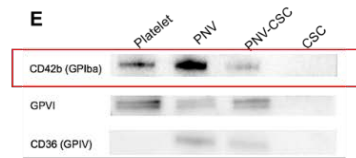
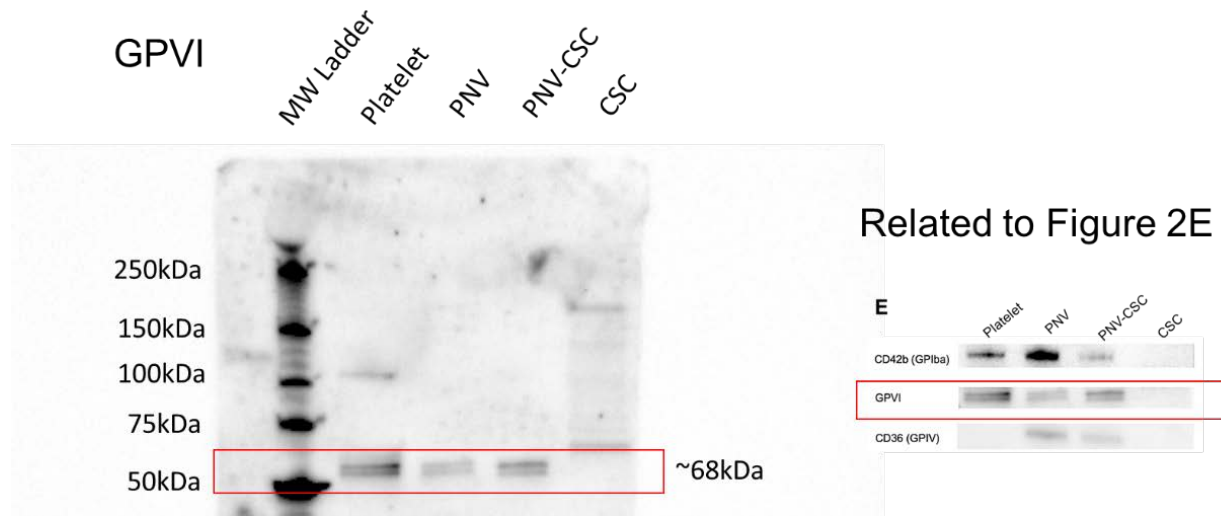myocardial tissue explant   cardiospheres   cardiosphere-derived cells

200 μm   200 μm   200 μm

Supplementary Figure 1. Rat CSCs derived using the cardiosphere method.

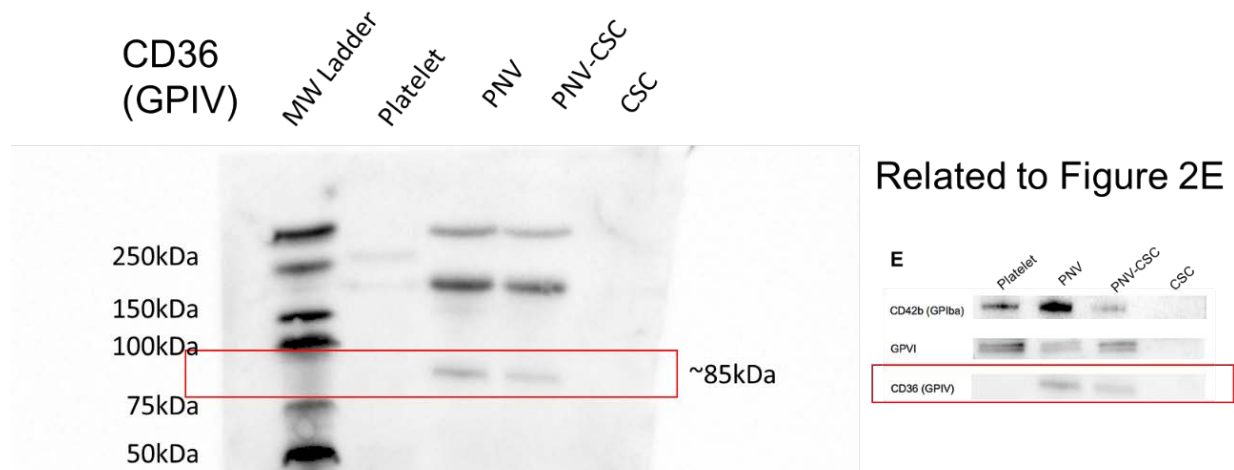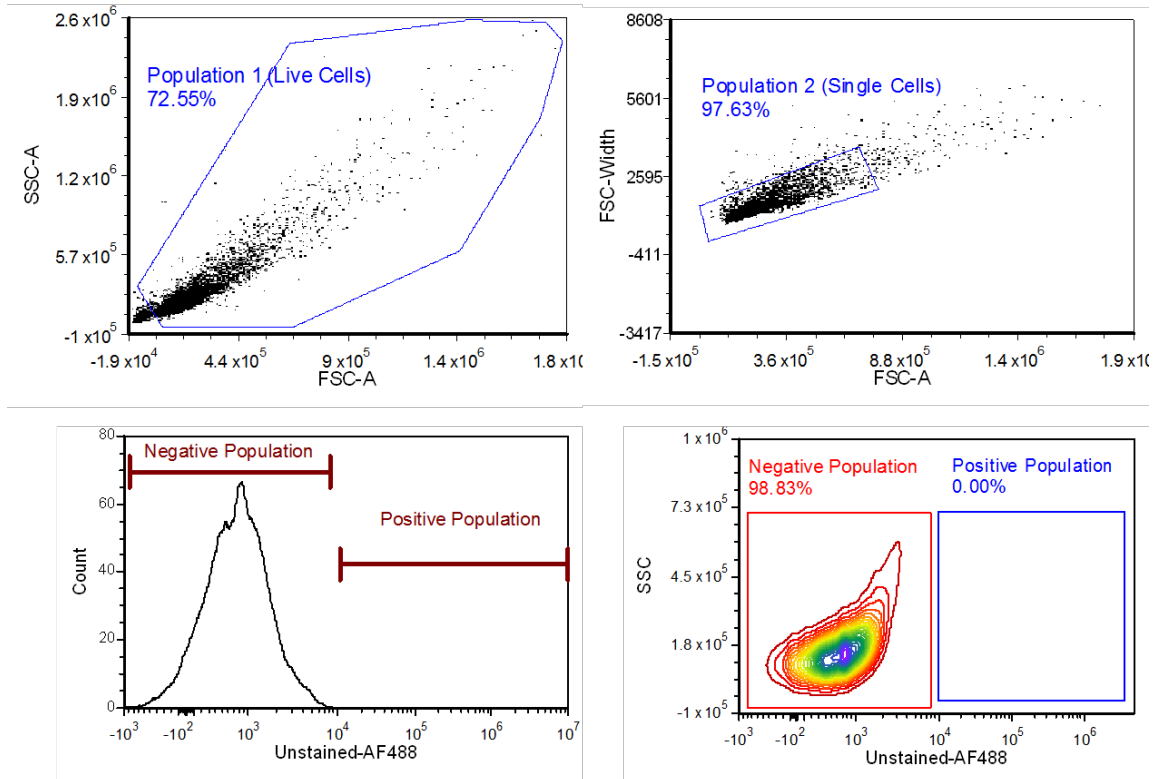**Supplementary Figure 2. Western blot analysis of CD42b in PNV-CSCs.**

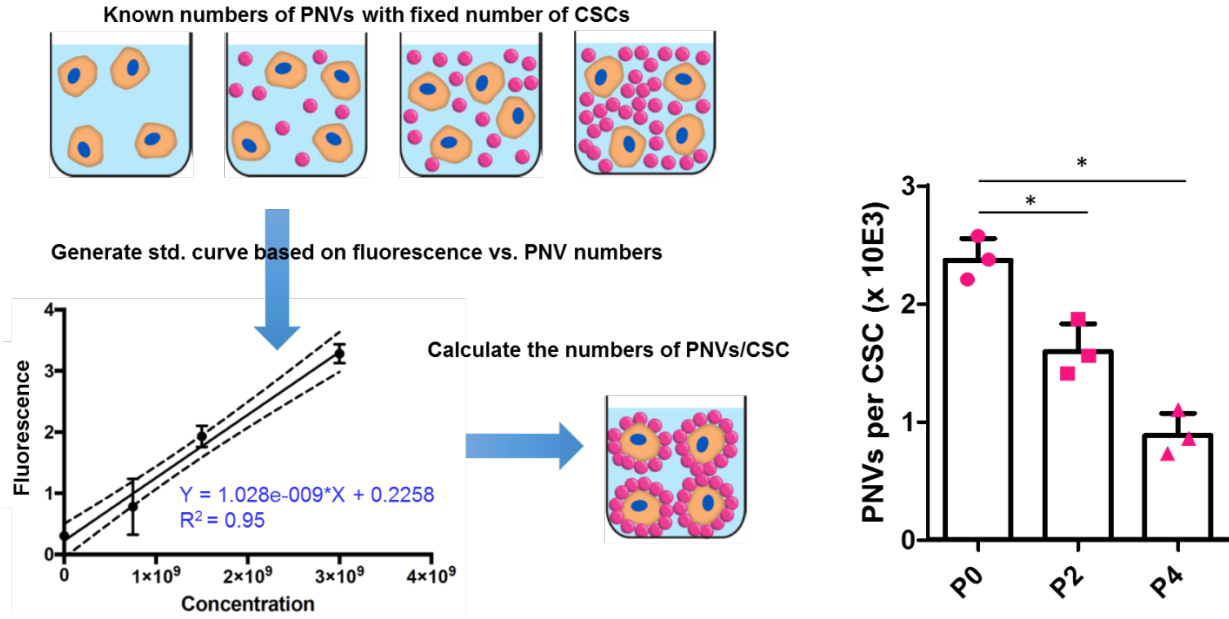**Supplementary Figure 3. Western blot analysis of GPVI in PNV-CSCs.**

Supplementary Figure 4. Western blot analysis of CD36(GPIV) in PNV-CSCs.

# Flow Cytometry Gating Strategy

Supplementary Figure 5. Flow cytometry gating strategies.

Supplementary Figure 6. Estimate of PNV coating efficiency. A standard curve was generated by mixing known numbers of DiI-labeled PNVs (pink) with unlabeled CSCs (orange). The fluorescence intensity was determined by a Tecan plate reader. Linear regression was performed to determine the relationship between the fluorescence intensity and the number of PNVs. Values are mean ± s.d. N =3 for each experiment. * Indicates $p < 0.05$ when compared to the "P0" group. Comparisons were performed using one-way ANOVA followed by post-hoc Bonferroni test.

Rate of Absorbance Change

PPP = platelet poor plasma
C = CSC
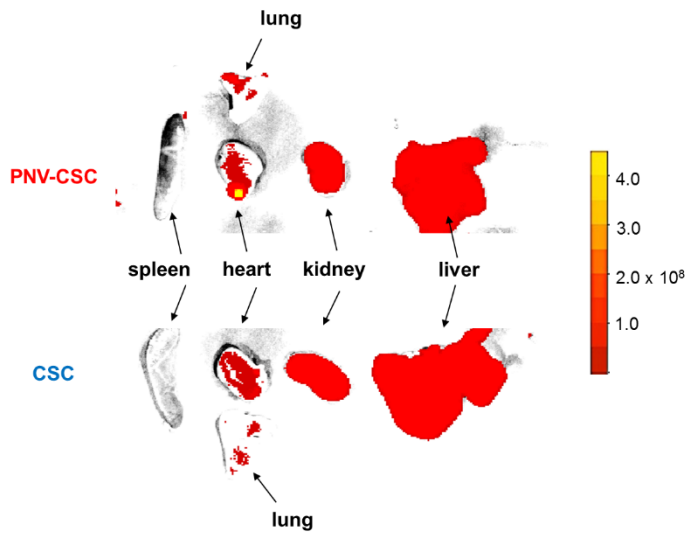P = PNV-CSC
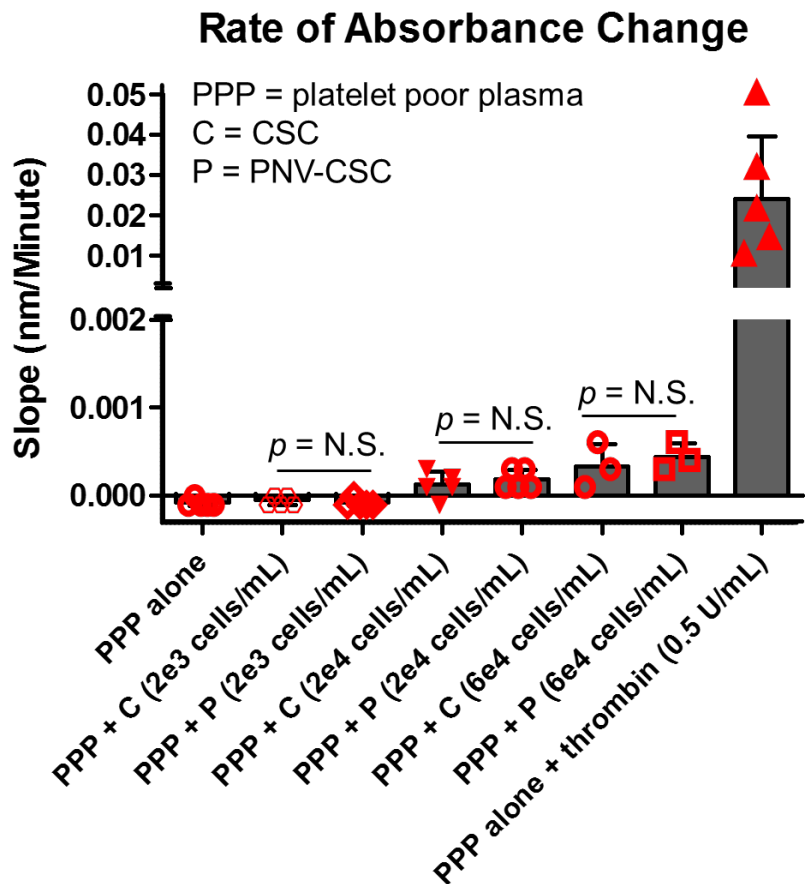
Supplementary Figure 7. Pro-thrombotic assay. To determine if PNV-decoration induced any adverse pro-thrombotic effects, polymerization of human platelet poor plasma (PPP) was analyzed in the absence or presence of control (undecorated) CSCs and PNV-CSCs. Samples were prepared to contain 85% PPP, 5% control CSCs, PNV-CSCs, or ultrapure water, and 10% $CaCl_2$ in ultrapure water. Three doses of CSCs or PNV-CSCs (2×10^3, 2×10^4, or 6×10^4 cells/mL) were used. $CaCl_2$ was used at a final concentration of 5 mM. Immediately following mixing, samples were transferred to a 96 well plate and polymerization was monitored by measuring absorbance at 350 nm every minute for 2 hours; as the clot polymerizes absorbance increases. The slope of the curve can be used to determine the rate of clot polymerization. Baseline absorbance readings were subtracted from readings and the linear portion of the polymerization curves were fit using linear regression in order to determine the slope. The slope corresponds to the rate of polymerization and is expressed in (nm/minute). N=3 for 6×10^4 cells/mL samples. N=5 for all other samples. Values are mean ± s.d. Two-tailed t test for comparison. N.S. indicates $p > 0.05$.
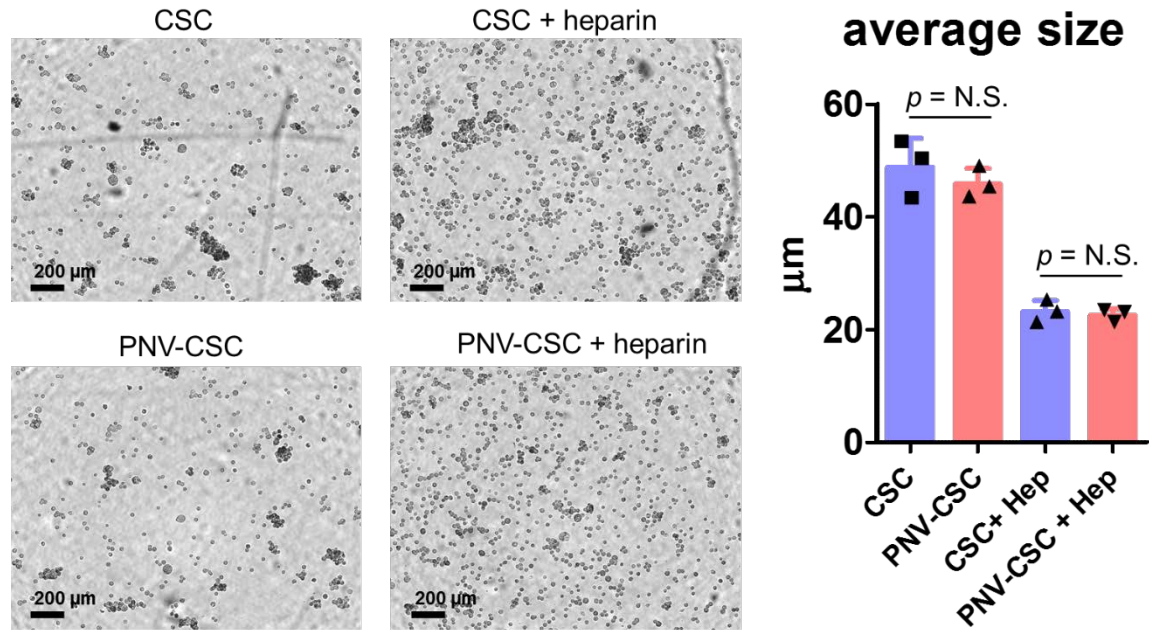
Supplementary Figure 8. Cell aggregation assay. PNV-CSCs and CSCs were stored in PBS with or without 100 U/mL Heparin at 4 °C for 24 hours. Cell clumping was analyzed under a microscope. N = 3 per group. All data are mean ± s.d. Comparisons were performed using one-way ANOVA followed by post-hoc Bonferroni test. N.S. indicates $p > 0.05$.
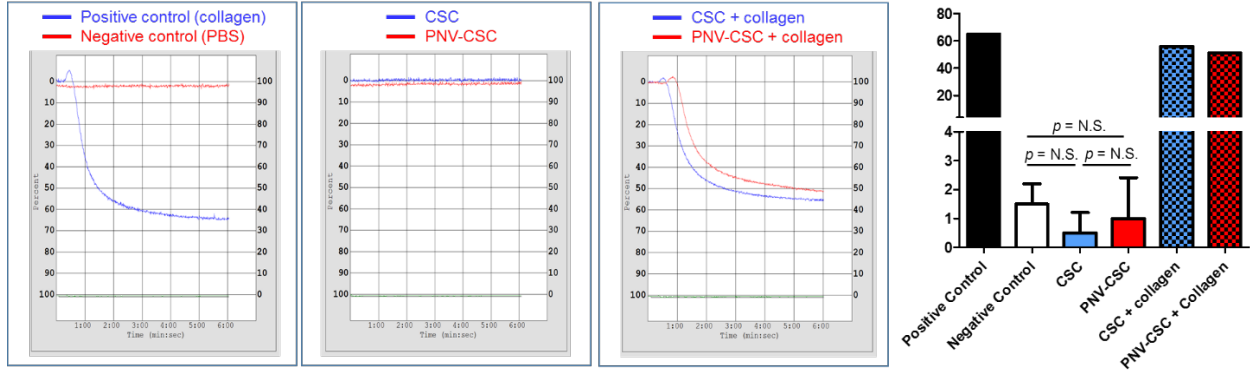
Supplementary Figure 9. Aggregometry assay for systemic pro-thrombotic risk of PNV-CSCs. Platelet rich plasma (PRP) was harvested from rats and mixed with collagen (black bar, as positive control), PBS (white bar, as negative control), CSCs or PNV-CSCs without collagen (blue and red bars) and CSCs or PNV-CSCs with collagen (blue and red dotted bars). N = 1 per group for "positive control", "CSC + collagen", and "PNV-CSC + collagen". N =2 per group for "negative control", "CSC", and "PNV-CSC". All data are mean ± s.d. N.S. indicates $p > 0.05$. Two tailed t test for comparison.

Supplementary Figure 10. Biodistribution of PNV-CSCs and CSCs 24 hrs after intracoronary delivery in rats with MI.
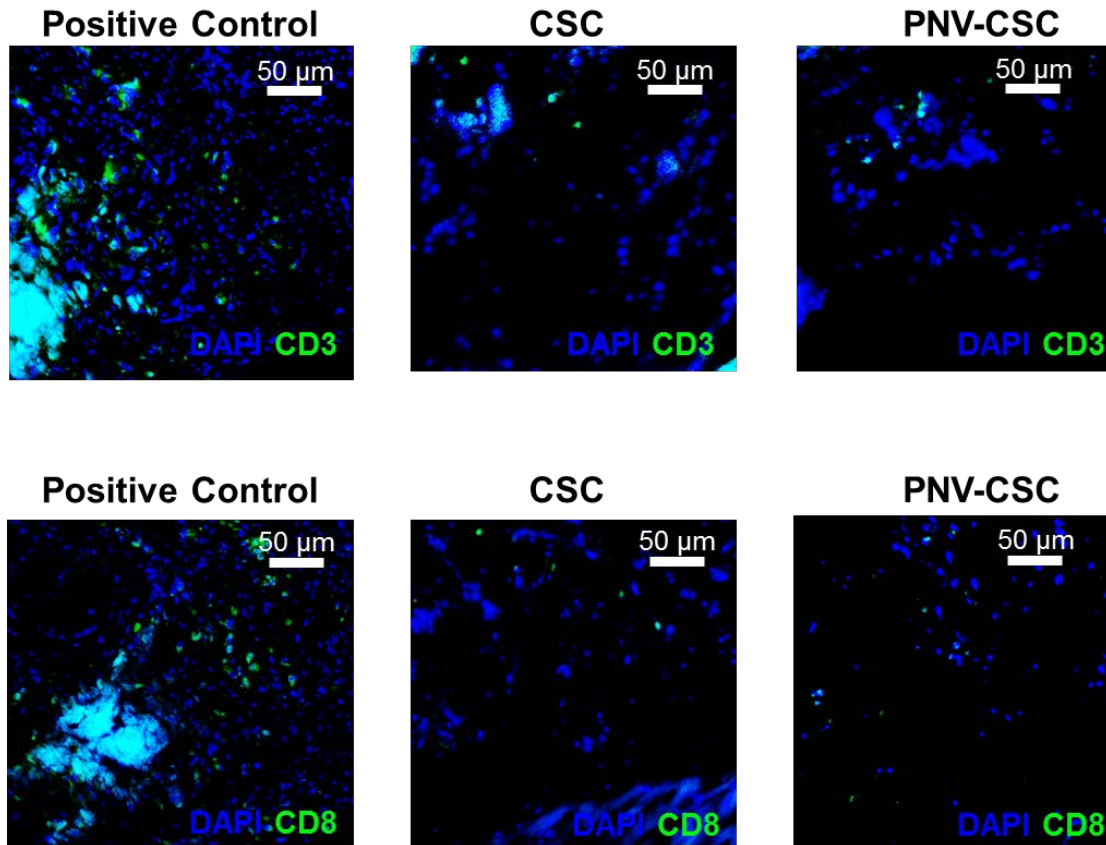
Supplementary Figure 11. Immunoresponse to PNV-CSC or CSC injections. 4 weeks after the therapy, only a negligible amount of CD3- and CD8-positive T cells could be detected in CSC- or PNV-CSC-treated hearts, while the positive control group (hearts injected with human CSCs) exhibited severe T cell infiltration (green).
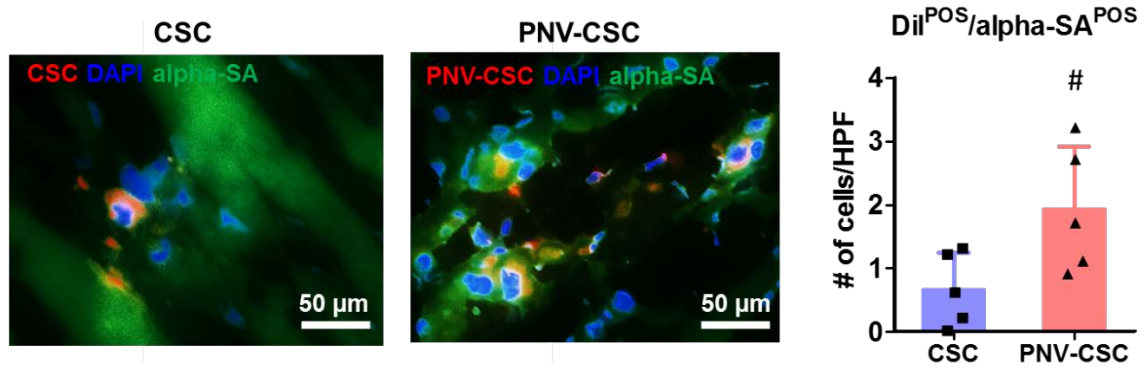
Supplementary Figure 12. Long-term engraftment and differentiation of injected CSCs.
N=5 animals per group. Values are mean ± s.d. Two-tailed *t* test for comparison. # indicates *p* <
0.05.

Cell retention by qPCR
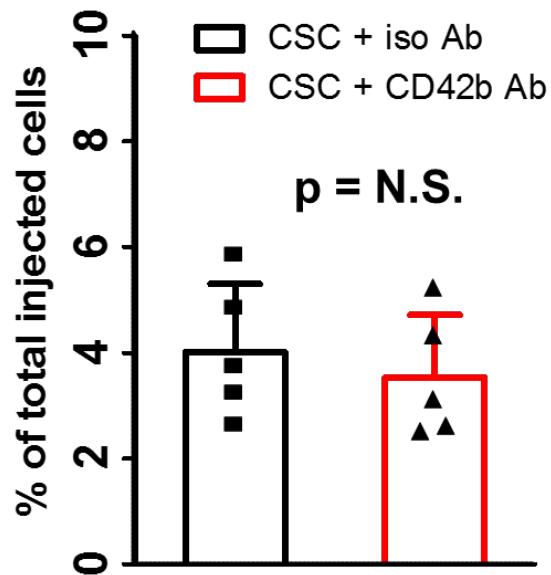
Supplementary Figure 13. Effects of CD42b blocking on CSC retention. N=5 animals per group. Values are mean ± s.d. Two-tailed *t* test for comparison. Quantitative PCR was performed on hearts 24 hrs post treatment. N.S. indicates *p* > 0.05.
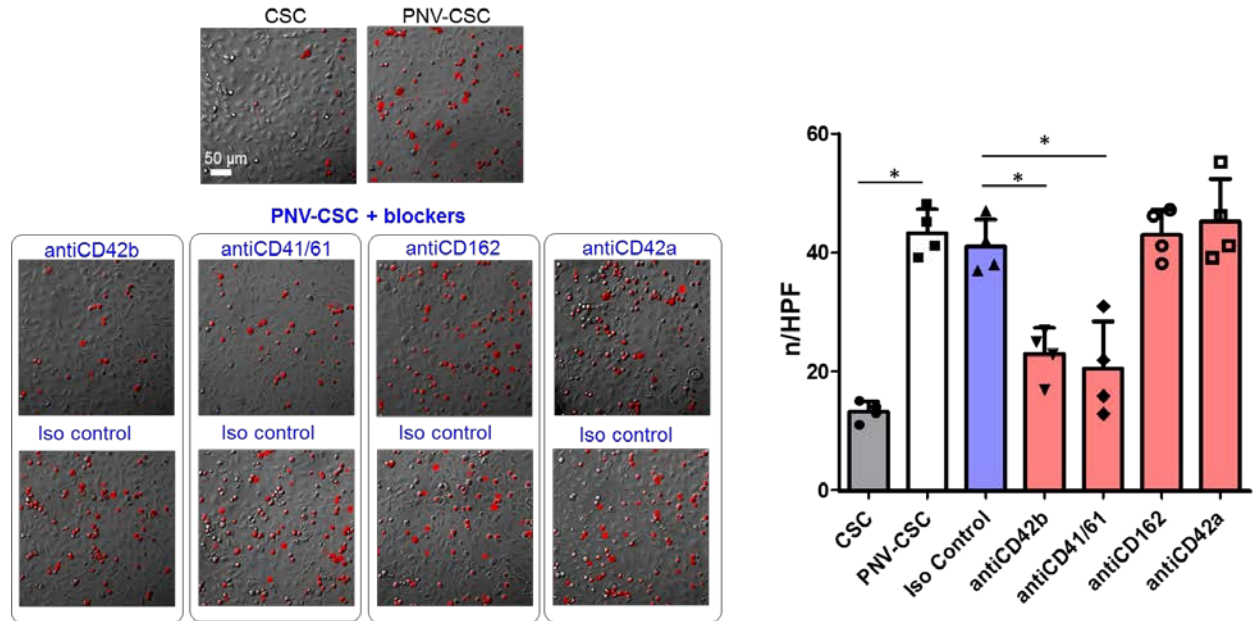
Supplementary Figure 14. Effects of CD42b, CD41/61, CD162, or CD42a blockage on PNV-CSC adhesion to endothelial cells. N=4 per group. Values are mean ± s.d. Two-tailed *t* test for comparison. * indicates *p* < 0.05 when compared to the CSC or Iso Control group.

Supplementary Table 1

Forward primer	5'-GGA GAG AGG CAC AAG TTG GC-3'
Reverse primer	5'-TCC CAG CTG CTT GCT GAT C-3'

Supplementary Movie 1. Angiogram showing blood flow before ischemia.

Supplementary Movie 2. Angiogram showing the location of balloon inflation and blood flow during ischemia.

Supplementary Movie 3. Angiogram showing blood flow after ischemia.